ELECTRONIC BEHAVIOR AND STATE CHANGES DRIVE ALL-THIN-FILM ELECTROCHROMIC DEVICE FOR ULTRA-LOW ENERGY CONSUMPTION SMART WINDOW

Haigang Yang[1], Xiaoling Song[1], Zichun Li[1], Hongyu Ma[1], Guoliang Ding[1], Guilin Song[2], Yong Zhang[1,]*
[1]College of Physics and Engineering Technology, Tonghua Normal University, Tonghua 134001, China
[2]School of Physics, Henan Province Advanced Semiconductor and Functional Device Integration Laboratory, Henan Normal University, Xinxiang 453000, China
**Email: yongzhang@thnu.edu.cn*

Abstract - Electrochromic smart windows can dynamically adjust the solar energy transmission rate under the influence of climate and seasonal changes, driven by a lower voltage. This significantly reduces the energy consumption of the temperature control system and can be applied to energy-saving lighting systems in buildings and vehicles. This is of great significance in terms of reducing energy consumption and cutting carbon emissions. In this work, a Glass/ITO/WO3/LiBSO/Ni1-xO/ITO all-thin-film electrochromic smart window device was fabricated on a single-layer substrate by magnetron sputtering method. The surface morphology, cross-sectional structure, and film thickness of the films were characterized by SEM. The influence of film deposition process, substrate temperature, and target-substrate distance during the fabrication of the smart window device on the electrochromic coloration range was investigated using visible light transmission spectra. The research results show that the thermal bombardment effect of the deposited particles during the film deposition process has a significant impact on the performance of the device. By reducing the substrate temperature during the film deposition process and increasing the distance between the target and the substrate, the electrochromic performance of the electrochromic smart window can be optimized.

Keywords: Electrochromic device, All-thin-film, Magnetron sputtering, Transmittance adjustment, Smart window.

1. Introduction

In the current era of rapid economic development and people's pursuit of a comfortable lifestyle, the issue of energy has become a matter of great concern for all countries. On the one hand, people are seeking to develop new energy sources; on the other hand, they are also exploring ways to efficiently utilize and conserve energy. For many workplaces and living areas, the energy consumption for temperature regulation during certain seasons can sometimes account for over 50% of the total energy usage. This is because the radiant heat passing through transparent windows, ceilings, and other structures exchanges heat with the outside, causing the air conditioning systems to operate at high loads. Electrochromic smart windows can dynamically alter the color state of the window under a relatively small voltage drive, thereby regulating the transmission rate of light radiation. To a certain extent, this can achieve the purpose of controlling indoor temperature and reduce the energy consumption of the air conditioning system [1-3]. In addition, the electrochromic device has a series of characteristics such as continuous adjustable modulation performance of transmitted light, multi-color display, low working voltage, low energy consumption, no radiation, wide viewing angle, and open-circuit memory. It has important application prospects in high-contrast non-radiative information display devices, active optical filters, and adjustable reflectivity rear-view mirrors for automobiles, as well as other information display and transmission devices [4-6].

Electrochromic smart windows can be classified into solid-liquid state, solid-gel state and all-solid state based on their structure. Among them, the smart windows with all-solid state structure have higher practical value [7-9]. At present, most of the applied electrochromic smart windows are

dx.doi.org/10.17683/ijomam/issue25/v1.17

sandwich-type solid-state devices. Due to the structure of these devices, which is composed of two substrate layers laminated together, they encounter significant limitations when applied in large areas and on curved surfaces [10-11]. Therefore, it is necessary to develop single-panel electrochromic intelligent windows. The structural feature of single-panel intelligent windows is that they are composed of five layers of films, belonging to all-solid-state electrochromic windows, also known as all-thin-film electrochromic windows. These smart windows also have advantages such as simple structure, anti-aging performance, and stable performance [12-15]. Preparing all-film electrochromic devices presents significant challenges. Due to the numerous factors affecting the performance of electrochromic devices, it is necessary to optimize the preparation parameters of each layer of the film, thereby optimizing its optical, electrical, and electrochromic properties. Moreover, the mutual influence between each film layer during the deposition process must be considered, which greatly increases the complexity of process parameter optimization and performance analysis. Therefore, there are not many reports on the preparation of all-thin-film electrochromic devices and their performance studies.

In this work, an all-thin-film electrochromic smart window device (ATF-ESWD) was successfully fabricated using a single magnetron sputtering method. The smart window consists of a glass substrate and five functional films. The five films are respectively a transparent conductive film, an electrochromic film, an ionic conductive film, an ionic storage film and a transparent conductive film. The structure is shown in Figure 1. The electrochromic film material is WO_3; the ionic conductive film material is LiBSO; the ionic storage film material is $Ni_{1-x}O$. Since the $Ni_{1-x}O$ film also has the anode coloring property, it also plays a complementary coloring role. The transparent conductive film is ITO. The effects of thin film deposition process, substrate temperature, target-substrate distance and other conditions on the performance of electrochromic smart windows were studied.

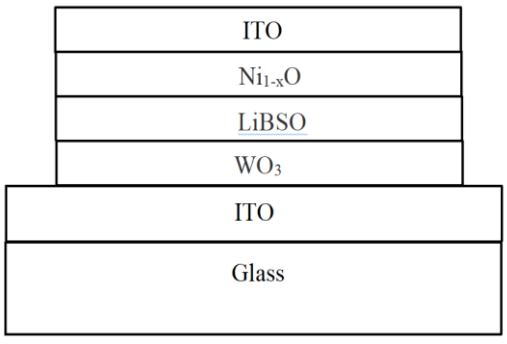

Figure 1: Structure diagram of ATF-ESWD

2. Experimental

2.1 Materials

The target materials used in this work include tungsten, nickel, ITO, and LIBSO targets, all with a diameter of 60 mm and a thickness of 3 mm. Tungsten and nickel targets were metal targets with a purity of 99.99%, while the ITO target was an In_2O_3-SnO_2 composite ceramic target (weight ratio of 90:10). All these targets were purchased from the Beijing General Research Institute for Nonferrous Metals. The LiBSO target was self-prepared using raw materials of $LiBO_2 \bullet 8H_2O$ and $Li_2SO_4 \bullet H_2O$ (analytical grade, provided by Sinopharm Chemical Reagent Co., Ltd.). First, the raw materials were dried at 90 °C in an oven. Then, they were ground uniformly in a molar ratio of $LiBO_2$ to Li_2SO_4 of 3:7, followed by adding an appropriate amount of polyvinyl alcohol [16]. The mixture was cold-pressed into shape using a 60 cm diameter mold, then dried at 100 °C in the oven to o allow water and organic substances to evaporate. Finally, the sample was sintered at 650 °C for 5 hours in a muffle furnace, resulting in a LiBSO ceramic target.

2.2 The Cooling Method for Substrate Temperature

In this work, the method of cooling the substrate with liquid nitrogen was adopted to fabricate devices composed of multiple layers of films under low-temperature conditions. The schematic diagram of the liquid nitrogen-cooled substrate device designed by ourselves is shown in Figure 2. The main components of the liquid nitrogen cooling device are: substrate cooling chamber, liquid nitrogen introduction pipe of the chamber, liquid nitrogen introduction flow control valve, liquid nitrogen cylinder, high-pressure nitrogen gas conduit, mass flow controller, high-pressure nitrogen cylinder, etc. The substrate cooling method is as follows: The substrate is closely attached to the surface of the cooling chamber. By adjusting the flow rate of nitrogen gas introduced from the nitrogen cylinder into the sealed liquid nitrogen cylinder, a certain pressure is maintained above the liquid nitrogen surface in the liquid nitrogen cylinder. The liquid nitrogen is then pushed into the substrate cooling chamber. The flow rate of liquid nitrogen entering the cooling chamber can be adjusted to achieve the purpose of low-temperature cooling of the substrate. Due to the difficulty in precisely measuring the temperature of the substrate surface located within the coated wall, we control the temperature of the substrate by measuring the temperature of the exhaust port of the cooling chamber.

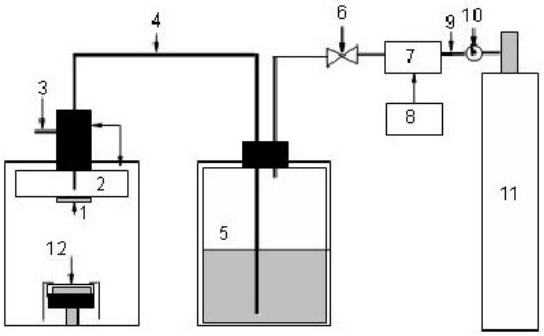

Figure 2: Liquid Nitrogen Cooling Substrate Device Structure Diagram: 1. Substrate, 2. Substrate cooling chamber, 3. Exhaust outlet of cooling chamber, 4. Liquid nitrogen introduction pipe of cooling chamber, 5. Liquid nitrogen cylinder, 6. Liquid nitrogen introduction flow control valve, 7. Mass flow controller, 8. Flow indicator, 9. High-pressure nitrogen outlet pipe, 10. Nitrogen cylinder pressure gauge, 11. High-pressure nitrogen cylinder, 12. Target material

2.3 Preparation of films and devices

The magnetron sputtering equipment used in this work is the GPJ-560 ultra-high vacuum magnetron sputtering system produced by the Shenyang Vacuum Science Instrument Factory of the Chinese Academy of Sciences.

The original substrate water cooling system of this equipment has been modified into a liquid nitrogen cooling system. The substrate used in the experiment was a purchased glass substrate coated with ITO transparent conductive film (surface resistance: 20Ω/□; Shijiazhuang Haowei Optoelectronic Film Technology Co., Ltd.). The preparation of ATF-ESWD is achieved by sequentially depositing WO_3, LiBSO, $Ni_{1-x}O$ and ITO films on an ITO substrate using DC sputtering or RF sputtering methods. The distance between the target material and the substrate was maintained at 6-7 cm, and the background pressure of the vacuum chamber was lower than 3×10^{-4} Pa. Before each film deposition, the target material is pre-sputtered in an argon atmosphere for 15 minutes to remove the impurities absorbed on the surface of the target. The sputtering gas is composed of argon and oxygen. They are introduced into the sputtering chamber as the sputtering gas and the reaction gas respectively. The sputtering pressure is 1 Pa or 3 Pa, and the sputtering power is 60 W, 90 W and 100 W. Different films have different deposition rates ranging from 4.5 to 35 nm/min due to variations in the target material, sputtering pressure, and sputtering power. By controlling the deposition time of the films, specific thicknesses of the films can be obtained. The deposition conditions for all functional layers of the ATF-ESWD are summarized in Table 1.

Table 1. Deposition conditions for the ATF-ESWD multilayer

Films	Sputtering type	Pressure (Pa)	Power (W)	Target material	Flow rates of gas (sccm)		Deposition rate (nm/min)
					Ar	O_2	
WO_3	DC	3	100	W	70	30	7.5
LiBSO	RF	1	60	LiBSO	90	10	4.5
$Ni_{1-x}O$	DC	3	90	Ni	70	30	35
ITO	RF	1	60	In_2O_3:SnO_2 (90:10 wt%)	50	0	6

2.4 Methods of Characterization

The morphology of the device surface and sectional structure was analyzed by a FEI Sirion SEM at 10 kV. The thicknesses of the films were determined from the SEM cross-section images. Electrochromic performance was tested by applying a 3 V voltage between the top and bottom electrodes of the device. The polarity of the electrodes was switched to cycle the device through its original, colored, and bleached states. The visible light transmittance spectrum of the sample was then measured using a Hitachi U-3010 UV-Vis spectrophotometer. By calculating the average through integration, we obtained the average transmittance values of the device in different states across the 400–800 nm wavelength range.

3. Results and Discussion

3.1 Structural Characterization of Electrochromic Smart Windows

Figure 3 shows the surface morphology of the ATF-ESWD. As can be seen that the surface of the device is relatively flat, and the outer ITO is composed of spherical particles, the size of these particles is about 40 nm.

The spherical particles of ITO indicate that its crystallinity is not very complete, which is due to the relatively low deposition temperature [17-18].

The test results show that the sheet resistance of the outer ITO film is 150 Ω/□ .

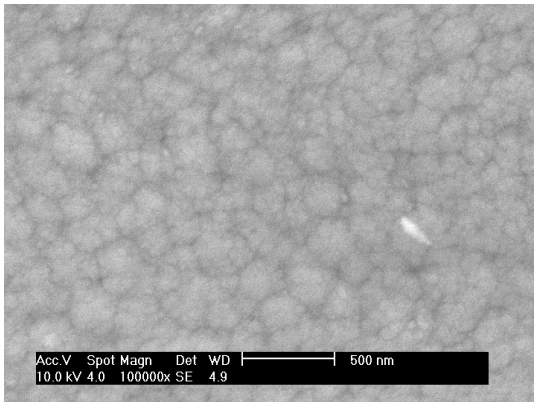

Figure 3: The surface morphology of the ATF-ESWD

Figure 4 shows a cross-sectional structure of the ATF-ESWD. As can be seen from the figure, the cross-sectional structural features of the five-layer film that constitutes the device. The results of the scale measurement indicate that the thickness of the ITO film on the glass substrate is 35 nm, the thickness of WO_3 film is 200 nm, the thickness of LiBSO film is 270 nm, the thickness of $Ni_{1-x}O$ film is 305 nm, and thickness of outer layer ITO film is 319 nm. The cross-sectional diagram also indicates that the internal structure of the outer ITO layer and the $Ni_{1-x}O$ layer presents a columnar feature. This is because during the deposition process of the particles and the formation of the film, the low substrate temperature inhibited the migration of the particles on the substrate surface, resulting in a relatively loose microstructure of the film [19-22]. The structure of the WO_3 film does not show any obvious loose features. This is because during the deposition of LiBSO, $Ni_{1-x}O$ and ITO films, the continuous bombardment of the deposited particles causes the structure to become more compact [23-26].

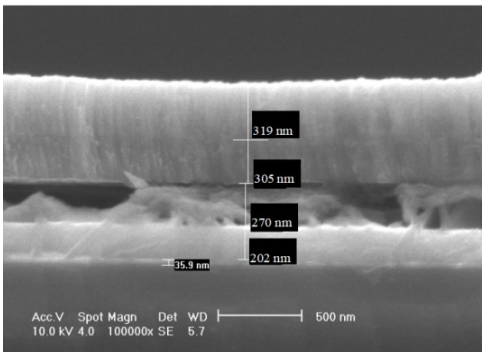

Figure 4: The cross-sectional structure of the ATF-ESWD

3.2 The impact of substrate temperature on the performance of ATF-ESWD

There have been previous studies on the influence of substrate temperature on the performance of single-layer electrochromic materials [6,10,17-19]. The focus of this research is on the impact of substrate temperature on the performance of electrochromic smart windows composed of multiple layers of films. Based on the previous research, this work mainly discusses the performance characteristics of the electrochromic smart windows prepared at substrate temperatures of –60 °C and –120 °C [27-29].

In order to study the influence relationship of the multi-layer film preparation process on the overall performance of the entire component, first, three layers of films consisting of WO_3, LiBSO, and $Ni_{1-x}O$ were successively deposited on the ITO glass substrate. An aluminum foil was used instead of the outer ITO as the electrode, and the electrochromic performance of the four-layer film was tested. During the electrochromic performance test, the smart window devices undergoes an electrochemical reaction as described by the following formula to achieve the color-changing function [30,31]:

$$WO_3 \text{ (bleach state)} + yLi^+ + ye^- \leftrightarrow Li_yWO_3 \text{ (the coloring state)} \quad (1)$$

$$Ni_{1-x}O \text{ (colored state)} + zLi^+ + ze^- \leftrightarrow Li_zNi_{1-x}O \text{ (the bleach state)} \quad (2)$$

Figure 5 shows the electrochromic test transmission spectra of the Glass / ITO / WO_3 / LiBSO / $Ni_{1-x}O$ multilayer films prepared under substrate temperatures of -60 ℃ and -120 ℃. In Figure 5, the three spectral lines correspond to the transmission spectra of the device in the original state (O), bleached state (B), and colored state (C) respectively. As can be seen from the figure, both samples exhibit obvious electrochromic properties. For sample (a), the average transmission rate at the initial state was 40.19%. Since the WO_3 and LiBSO films were transparent at the initial state, the absorption of light mainly came from the $Ni_{1-x}O$ film. The color of the multilayer film device was light brown [32,33]. When the device is in the colored state, its average transmittance drops to 20.70%, which is due to the injection of Li^+ into the WO_3 film, causing some W^{6+} to be reduced to W^{5+}, resulting in the color of WO_3 changing to a dark blue [26, 31]. When the device is in the bleached state, its average transmission rate reaches 51.17%. This is because, on the one hand, the Li^+ ions in the colored WO_3 are extracted, and the W^{5+} ions are oxidized to W^{6+} to restore transparency. On the other hand, due to the injection of Li^+ into the $Ni_{1-x}O$ film, some Ni^{3+} is reduced to Ni^{2+}, and the color of $Ni_{1-x}O$ changes from light brown to transparent [21, 30]. From the previous analysis, it can be seen that the color-tuning range below the original color state transmittance mainly comes from the WO_3 film, corresponding to the electrochemical reaction in Equation (1), while the color-tuning range above the original color state transmittance mainly comes from the $Ni_{1-x}O$ film,

corresponding to the electrochemical reaction in Equation (2). From the electrochromic characteristics of the devices shown in Figures 4(a) and (b), it can also be concluded that for the devices prepared at a lower substrate temperature (b), the color-changing range from the WO_3 film layer has significantly increased, reaching 26.73%, while the color-changing increase from the $Ni_{1-x}O$ film layer is not as obvious. This is because at lower substrate temperatures, it is easier to obtain a loose structure of the WO_3 film, which is conducive to the migration of Li^+ in the film layer, and the WO_3 film layer has relatively strict requirements for the substrate temperature [13,17].

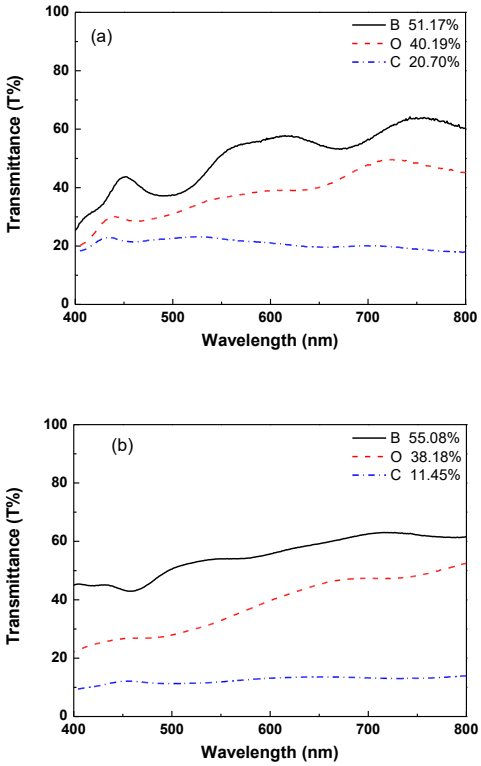

Figure 5: Spectral diagrams of the Glass / ITO / WO_3 / LiBSO / $Ni_{1-x}O$ devices fabricated under different substrate temperatures: (a) -60 ℃, (b) -120 ℃

Based on the successful preparation of the four-layer thin film device, we fabricated a five-layer thin film structure of Glass/ITO/WO_3/LiBSO/$Ni_{1-x}O$/ITO ATF-ESWD under substrate temperatures of -60 ℃ and -120 ℃, respectively. Figure 6 shows the electrochromic test transmission spectra of the ATF-ESWD. By analyzing Figures 6(a) and Figures 6(b), it can be observed that when the substrate temperature is -120 ℃, the transmittance of the fabricated device in the original state is relatively low. This is partly because, during the preparation of the $Ni_{1-x}O$ film, the lower substrate temperature limits the lateral migration of the deposited particles and reduces the energy required for the particles to combine into a film, resulting in a decrease in the crystallinity and density of the obtained $Ni_{1-x}O$ film. Furthermore, when the substrate temperature is low, there are more O molecules adsorbed on the substrate surface, which is conducive to obtaining a $Ni_{1-x}O$ film with an oxygen-rich structure, resulting in an increase in the content of Ni^{3+}. On the other hand, under conditions where the substrate temperature is low, when depositing the outer layer of ITO film, the energy from the thermal bombardment of the deposition particles on the $Ni_{1-x}O$ film is effectively dissipated, thereby effectively reducing the thermal bombardment effect of the deposition particles on the existing film [10,12,13].

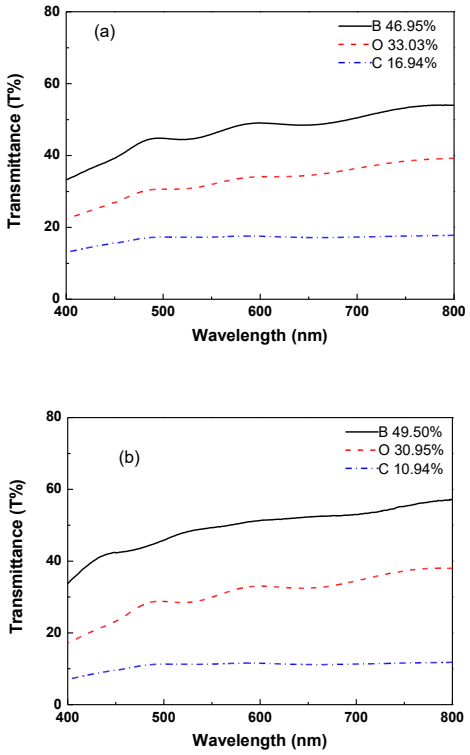

Figure 6: Spectral diagrams of the Glass / ITO / WO_3 / LiBSO / $Ni_{1-x}O$ / ITO devices fabricated under different substrate temperatures: (a) -60 ℃, (b) -120 ℃

3.3 The Influence of Target-substrate Distance on the Performance of ATF-ESWD

To further reduce the thermal bombardment effect of deposited particles on the existing films, when preparing the outer ITO layer, we investigated the influence of the target-substrate distance on the performance of the electrochromic device. The target-substrate distances during the fabrication processes of devices (a) and (b) in Figure 7 were 6 cm and 7 cm, respectively. Through the analysis of the electrochromic performance test, it is known that when the target-substrate distance is 6 cm, the color-tuning range of device (a) is 29.18% (47.76% -

18.58%). When the target-base distance is 7 cm, the color gamut of the device (b) is 31.52% (47.19% - 15.67%). The analysis results indicate that a larger target pitch distance is beneficial for enhancing the electrochromic coloration range of the device [10,13,21]. This is because when preparing the ITO film, under the condition of a large target-to-substrate distance, the deposited particles will undergo more scattering during their migration towards the substrate, resulting in lower energy of the deposited particles when they reach the substrate [12,13]. This reduces the thermal bombardment effect on the existing film. In related research, in order to reduce the influence of deposited ITO particles on the existing film, the outer ITO film is usually prepared by thermal evaporation technology [34,35]. It can also be observed from Figure 6 that when the target pitch is larger, the resulting device has a slightly lower transmittance in the bleached state. This is because when the energy of the ITO deposition particles is relatively low, the resulting ITO film has poorer density and crystallinity [17,19,20].

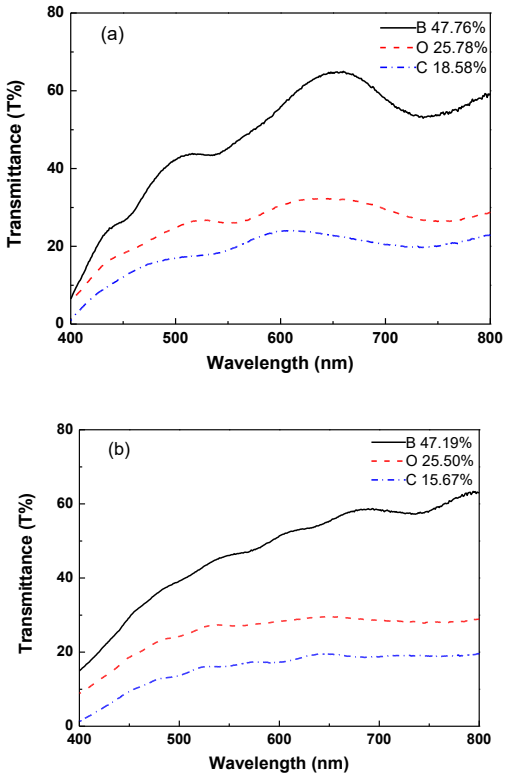

Figure 7: Spectral diagrams of the Glass / ITO / WO_3 / LiBSO / $Ni_{1-x}O$ / ITO devices fabricated under different target-substrate distance: (a)6 cm, (b)7 cm

4. Conclusions

In this work, a full-film electrochromic smart window device was successfully fabricated using a single magnetron sputtering technique. This device has the advantages of low raw material cost, simple fabrication process, and excellent performance.

The influence relationship of the preparation process of multilayer films on the overall performance of the entire device was studied. The research results indicate that during the film deposition process, the impact effect of the deposited particles on the existing film will affect the microstructure of the film, and subsequently influence the performance of the entire device. By reducing the substrate temperature during the film deposition process, on the one hand, it can inhibit the lateral migration of deposition particles, making it easier to obtain a porous film structure. This is beneficial for the easy migration of Li+ between the film layers. On the one hand, due to the decrease in substrate temperature, it can effectively reduce the accumulation effect of substrate heat caused by the thermal bombardment of deposited particles, thereby minimizing the impact on the microstructure of the existing film. Furthermore, by increasing the target distance during the film preparation process, the influence of the deposited particles on the thermal bombardment effect of the existing film can be further reduced. The electrochromic smart window device prepared in this work has an average coloration range of 38.6% in the visible light region, which can meet the practical application requirements. It has great application value in fields such as intelligent windows of buildings and energy-saving systems.

Acknowledgements

This work was supported by Scientific Research Project of the Department of Education of Jilin Province (JJKH20240644KJ).

References

[1] Leftheriotis G, Syrrokostas G, Yianoulis P. Development of photoelectrochromic devices for dynamic solar control in buildings. Solar Energy Materials & Solar Cells, 2010, 94(12):2304-2313.

[2] Tang Y, Yuan J, Zheng R, et al. Scalable Fabrication of Large-Scale Electrochromic Smart Windows for Superior Solar Radiation Regulation and Energy Savings. Nano-Micro Letters, 2026, 18(1).

[3] Bagheri-Esfeh H. Multi-objective optimization of electrochromic windows in office buildings for different climatic conditions. International Communications in Heat and Mass Transfer, 2025, 162(3):108669.

[4] Shi A, Yang G, Ghani A, et al. Crystal adjustment-based neutral-tinted nickel-tungsten-oxygen for electrochromic energy-efficient windows with wide spectral regulation. Chemical Engineering Journal, 2025, 509(4):161406.

[5] Crouan M, Baloukas B, Zabeida O, et al. Antireflective-to-mirror-like all-solid-state electrochromic devices. Optical Materials, 2025, 168(11):117464.
[6] Qu Z, Li X, Duan H, et al. Aging-induced hierarchically porous WOx films for high-performance electrochromic smart windows. Journal of Alloys and Compounds, 2026, 1053(2):186214.
[7] Zhang Y, Xiang S, Cheng B, et al. Nanocrystal-in-Glass Prussian Blue Thin Films for Quasi-Solid-State Electrochromic Devices with Long-Term Stability. Applied Materials Today,2024,43(4),102655.
[8] Zhang F, Ye J, Lu H, et al. Preparing and investigating the monolithically stacked flexible tandem all-thin-film electrochromic device. Opt. Mater. 2024,149 (3): 115115.
[9] Claes G, Granqvist. Electrochromics for smart windows: Oxide-based thin films and devices. Thin Solid Films: An International Journal on the Science and Technology of Thin and Thick Films, 2014,564 (2014): 1-38.
[10] Ding Y, Wang M, Mei Z, *et al*. Electrochromic Adaptability of NiOx Films Modified by Substrate Temperature in Aqueous and Non-Aqueous Electrolytes. Advanced Materials Interfaces,2022,9(17): 2102223.
[11] Granqvist C G. Oxide electrochromics: An introduction to devices and materials. Solar Energy Materials & Solar Cells, 2012, 99(4):1-13.
[12] Zhou C, Xu H, Wu K, et al. Lithium tantalate film prepared by RF magnetron sputtering and effect of thickness on performance of inorganic electrochromic devices. Ceramics International, 2025: 51 (5):5899-5905.
[13] West W C, Hood Z D, Adhikari S P, et al. Reduction of charge-transfer resistance at the solid electrolyte – electrode interface by pulsed laser deposition of films from a crystalline Li_2PO_2N source. Journal of Power Sources, 2016, 312(4):116-122.
[14] Gellert M, Gries K I, Zakel J, et al. Charge Transfer across the Interface between LiNi0.5Mn1.5O4 High-Voltage Cathode Films and Solid Electrolyte Films. Journal of the Electrochemical Society, 2015, 162(4): A754-A759.
[15] Ahlawat N, Bansal L, Sahu B, et al. Complementary Oxides Based Electrochromic Supercapacitor: Multiwavelength Switchable Solid State Device. ACS Applied Energy Materials, 2025, 8(7): 4288-4298.
[16] Joo K. H., Vinatier P., Pecquenard B., Thin film lithium ion conducting LiBSO solid electrolyte. Solid State Ionics, 2003, V160: 51-59.
[17] Zhang Y, Zhao L, Yang C, et al. Substrate temperature-controlled amorphous-crystalline hybrid structure in tungsten oxide thin films for comprehensive high-efficiency electrochromic performance. Surfaces and Interfaces, 2025, 72(10):107404.
[18] Zhang L, Li A, Chen Y, et al. Preparation of WO3 films by magnetron sputtering: Preparation process and influence of ZnO doping on the electrochromic properties of the films. Physica B: Condensed Matter, 2025, 702(4):416980.
[19] Chen M, Huang Z, Shiyu Z, et al. Tailoring NiOx thin film properties via reactive magnetron sputtering discharge power for high performance flexible all-thin-film electrochromic devices. Journal of Alloys and Compounds,2025:1039 (9): 183181.
[20] Gutpa J, Shaik H, Naveen K K, et al. PVD techniques proffering avenues for fabrication of porous tungsten oxide (WO3) thin films: A review. Materials science in semiconductor processing, 2022,:143(6):106534.
[21] Zhang L, Chen H, Li A, et al. Investigation of Peeling Mechanisms in NiO Electrochromic Thin Films and Strategies for Mitigation. Physica B: Condensed Matter, 2025,714(10):417398.
[22] Xu J, Li X, Zhang Y, et al. Effect of In Situ Heating on the Growth and Electrochromic Properties of Tungsten Trioxide Thin Films. Materials, 2024, 17(10):17102214.
[23] Atak G, Cokun Z D. Annealing effects of NiO thin films for all-solid-state electrochromic devices. Solid State Ionics, 2017: 305 (7) :43-51.
[24] Rong D, Gao J, Wang W, et al. Electrochromic laminated safety glass based on WO3 nanofilm with high optical modulation and quick response. Applied Surface Science, 2025, 688(4):162413.
[25] Fan X, Zhang C, Wang S, et al. Porous Electrochromic Structures: A Review. SmartMat, 2025, 6(5):70036.
[26] Junsukhon A, Ngaotrakanwiwat P, Tatsuma T. Visible and Near-Infrared Electrochromic Smart Windows with Amorphous WO3-x and Cu-Doped NiO Operating in Three Modes. Electrochemistry, 2025, 93(9):094007-094007.
[27] Yang H. G, Wang C, Diao X. G, et al. A new all-thin-film electrochromic device using LiBSO as the ion conducting layer. Journal of Physics D: Applied Physics. 2008,41(11):115301-115301.
[28] Yang H. G, Song, G L, Wang T X, et al. Electrochromic response time performance of NiOx film prepared by reactive sputtering. Acta Optica Sinica.2011, 31(5):0531003-0531003.
[29] Yang H. G, Hao R. T, Li M. C, et al. A novel all-thin-film electrochromic device for modulating optical transmittance. Bulgarian Chemical Communications.2018,50(2) :329-333.
[30] Gellert M, Gries K I, Sann J, et al. Impedance spectroscopic study of the charge transfer resistance at the interface between a LiNi0.5Mn1.5O4 high-voltage cathode film and a LiNbO3 coating film. Solid State Ionics, 2016, 287(4):8-12.

[31] Wang L, Zhang X, Li Y. A Novel Method for Performance Rejuvenation of WO3//NiO Electrochromic Devices: Lithium-Ion Kinetic Behavior with Variable Cycling Temperature and Switching Voltage. ACS Sustain. Chem. Eng. 2023,11 (37) :13566-13573.

[32] Liu J, Chen Y, Wang P, et al. Four-state electrochromic smart devices for dynamic environmental adaptive camouflage with synergistic thermal–electromagnetic energy management. Journal of Materials Chemistry C, 2026, 14(2):754-764.

[33] Haider I, Xu H, Haider S A, et al. Color-switchable phosphomolybdate-nickel nanofilm with superior optical modulation and long-term stability for electrochromic energy storage. Journal of Power Sources, 2025, 636(4):236578.

[34] Zhang L, Zhao M, Chen Y, et al. Effect of sputtering pressure on the electrochromic properties of flexible NiO films prepared by magnetron sputtering. Materials Letters, 2024, 354(1):135317.

[35] Rauf S. Dual radio frequency sources in a magnetized capacitively coupled plasma discharge. IEEE Transactions on Plasma Science, 2003, 31(4):471-478.